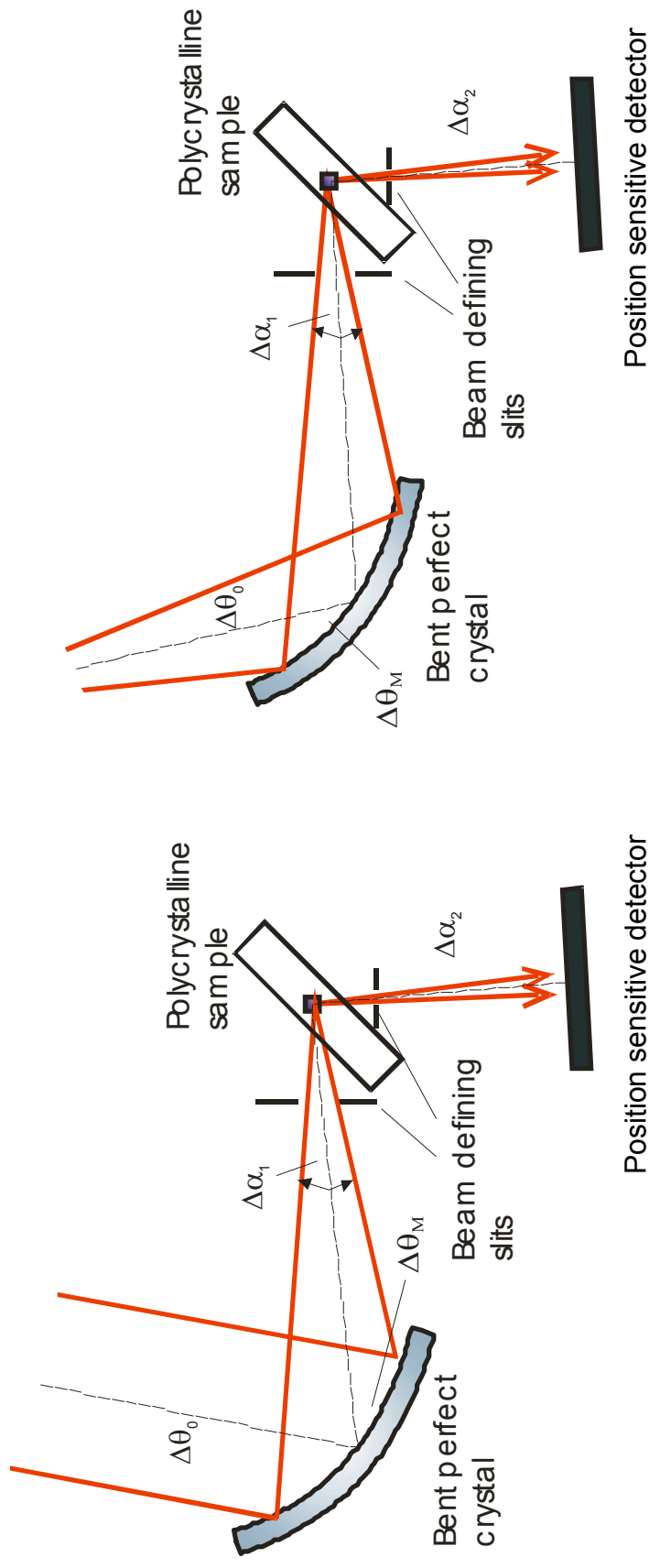


Bragg diffraction optics

NPI Řež, Czech Republic

NMI3 meeting, Rome, 2011

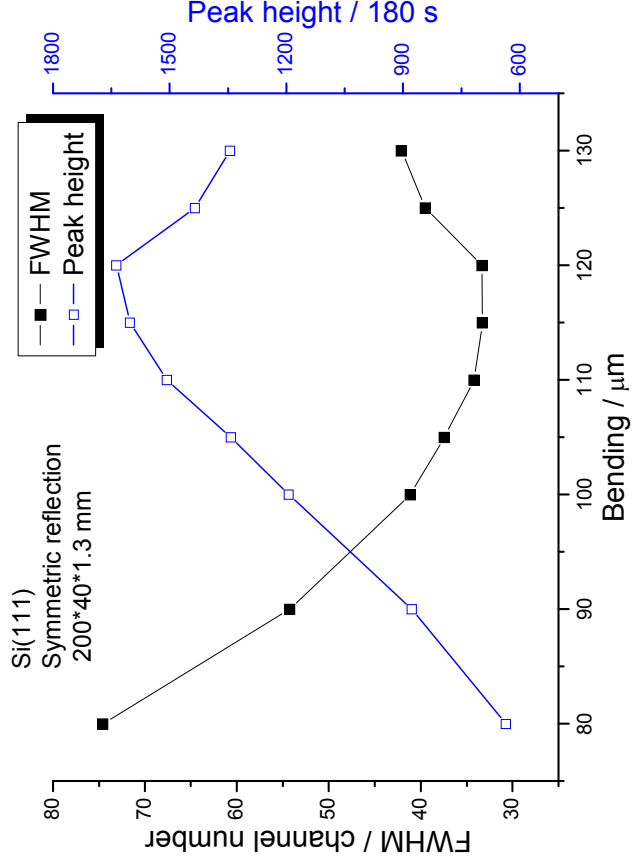
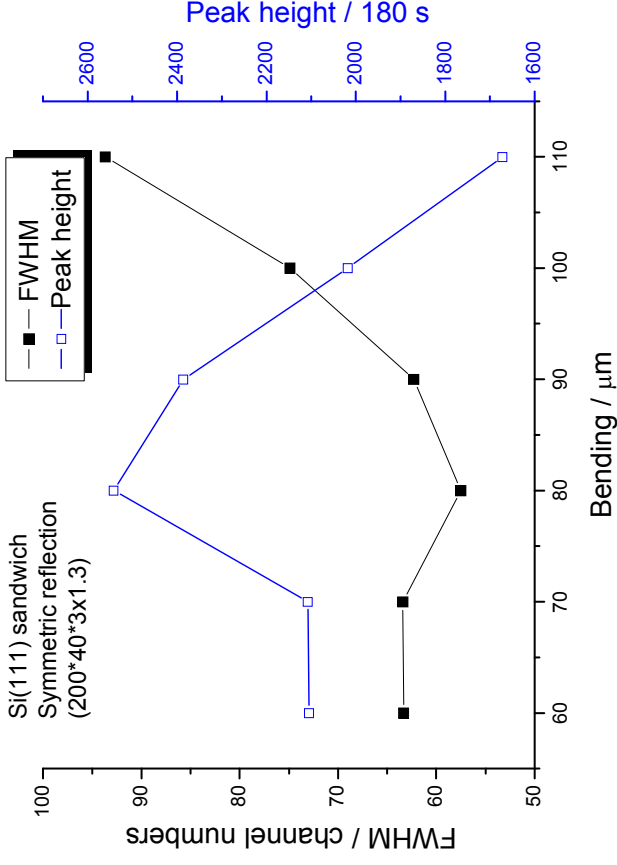
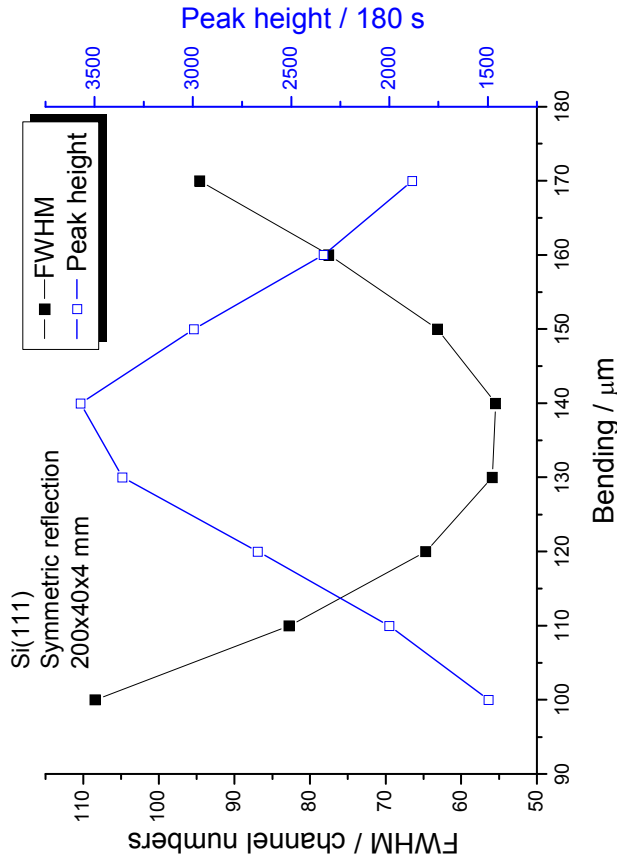
Focusing monochromator in the powder diffraction case



Schematic geometry of the usual focusing diffractometer performance with a large take-off angle (left) and the one tested in KAERI (right) with take-off angle $2\theta_M=30^\circ$ and $2\theta=90^\circ$.

Intensity delivered on the sample is proportional to $\Delta\lambda$ spread. However, $\Delta\lambda/\lambda = \Delta\theta \times \cot \theta$.

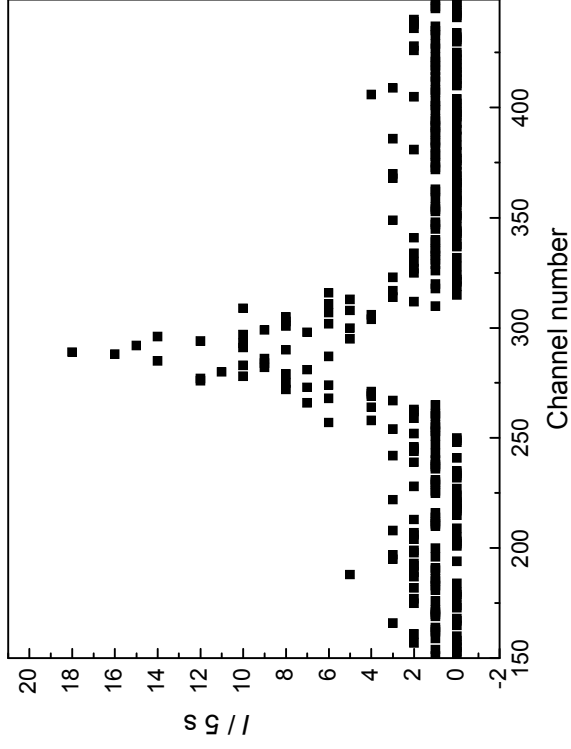
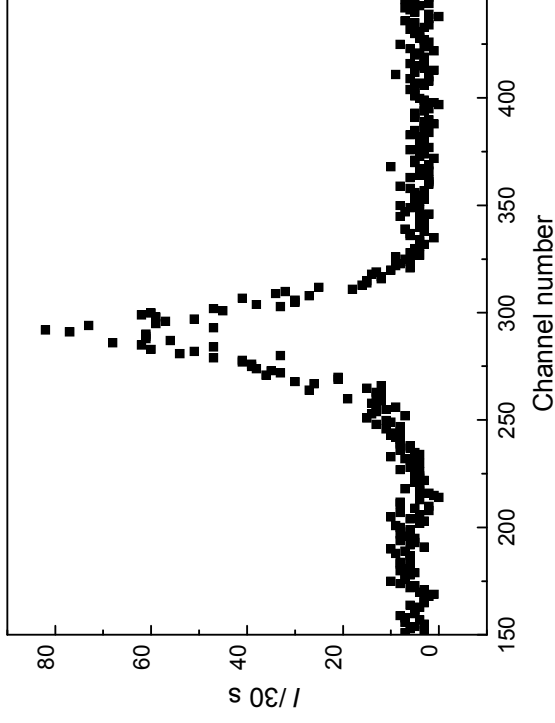
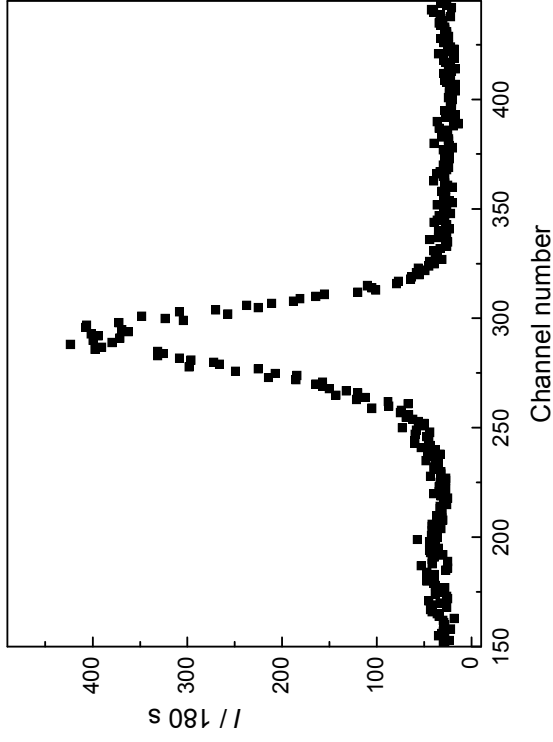
Experimental results: Symmetric reflection geometry



The luminosity and resolution characteristics of the strain/stress diffractometer performance for the focusing Si(111) monochromator of the thickness of 3.9 mm and 1.3 mm, α -Fe(211) steel pin of 2 mm diameter and 40 mm height, $2\theta_M = 30^\circ$, for $\lambda = 1.62 \text{ \AA}$ the scattering angle on the sample was $2\theta_S = 87.8^\circ$.

1 channel = 0.01°

Diffraction profiles for different measurement times

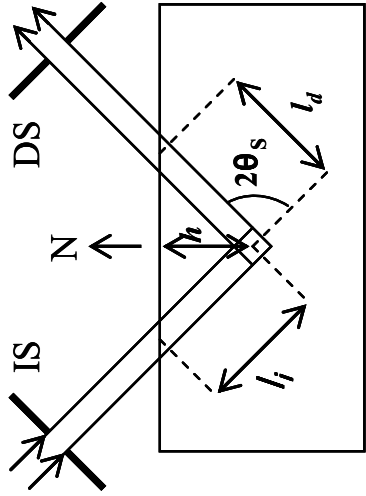


1 channel = 0.01°

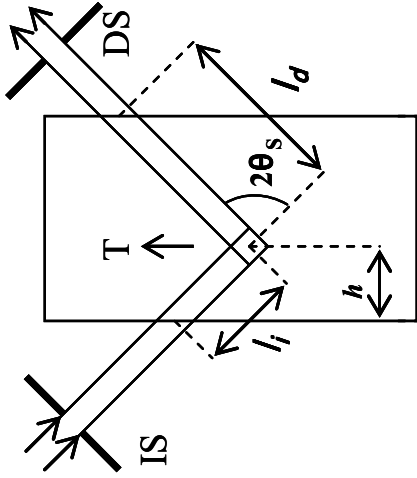
B.S. Seong, V. Em, P. Mikula, J. Šaroun, M.H. Kang, *Optimization of the bent perfect Si(111) monochromator, at small ($\sim 30^\circ$) take-off angle for stress instrument*, J. Appl. Cryst. **43** (2010) 654-658.

B.S. Seong, V. Em, P. Mikula, J. Šaroun, M.H. Kang, *Unconventional Performance of a Highly Luminous Strain/Stress Scanner for High Resolution Studies*, In Proc. Of the Int. Conf. ECRS8 held in Riva del Garda, June 26-28, 2010, Mat. Science Forum, Materials Science Forum Vol. **681** (2011) 426-430.

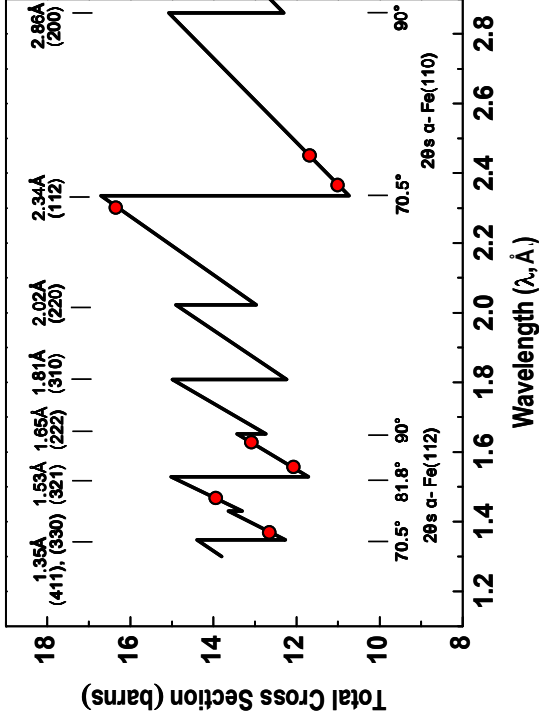
Strain/stress measurements at a large depth in steels



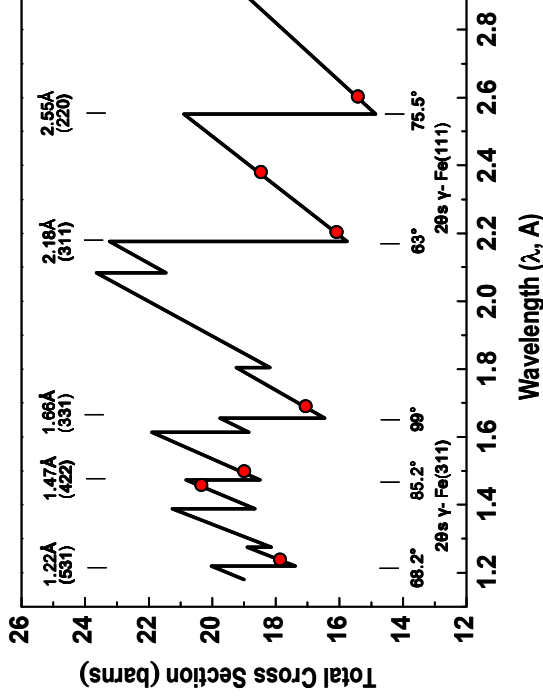
a) $l = l_i + l_d = 2h / \sin\theta$



b) $l = l_i + l_d = d / \cos\theta$



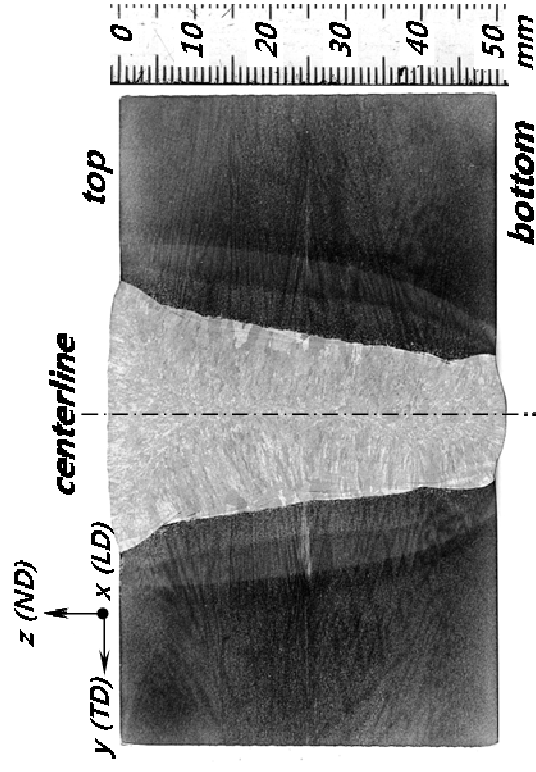
Total neutron cross-section of ferrite (α -Fe) as a function of wavelength. The wavelengths at which the maximum penetration depth was measured are shown with black closed circles.



Total neutron cross-section of austenite (γ -Fe) as a function of wavelength. The wavelengths at which the maximum penetration depth was measured are shown with black closed circles.

λ (Å)	$2\theta_{\text{monochromator}}$ (degree)	$2\theta_{\text{diffraction}}$ (degree)	Diffraction Peak	Total path length (mm)	Available thickness (mm)
1.80	90	90.0	211	40	28 (ref. 10)
2.28	43	68.5	110	64	36
2.39	45	72.4	110	83	50

Maximum total path length ($l_1 + l_2$) and available thickness (t) using the selected wavelength (λ) in the ferrite steel specimen based on $\pm 100 \mu\text{e}$ precision and 1 hour measurement time. Compared to the previous result measured with the wavelength of 1.80 Å

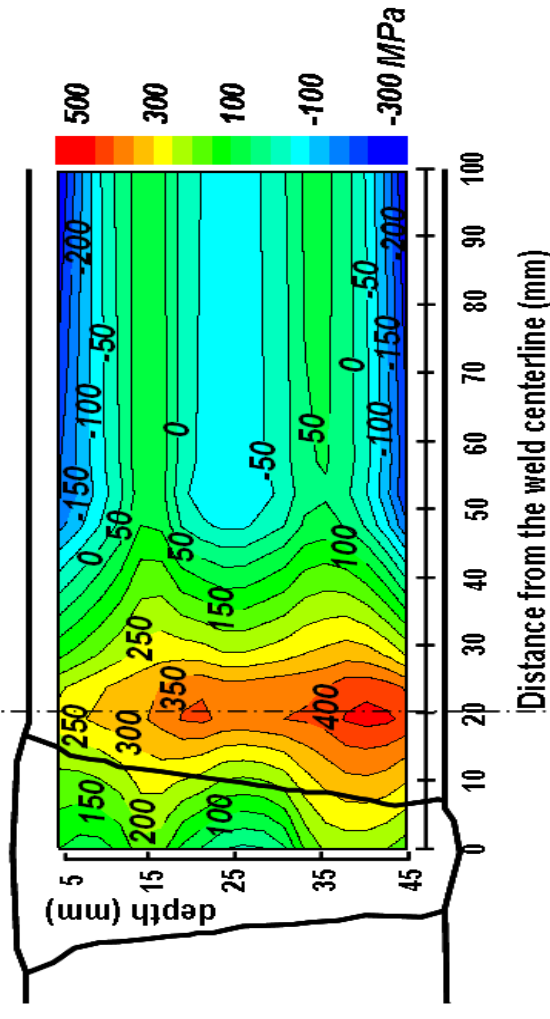


Macrostructure of the 50-mm thick low-carbon steel weld. Noted the LD (longitudinal, x), TD (transverse, y), and ND (normal, z) directions of the weld plate.

W. Woo, V. Em, B.S. Seong, E. Shin, P. Mikula, J. Joo and M.H. Kang, *Effect of wavelength-dependent attenuation on neutron diffraction stress measurements at depth in steels*, J. Appl. Cryst. **44** (2011) 747-754.

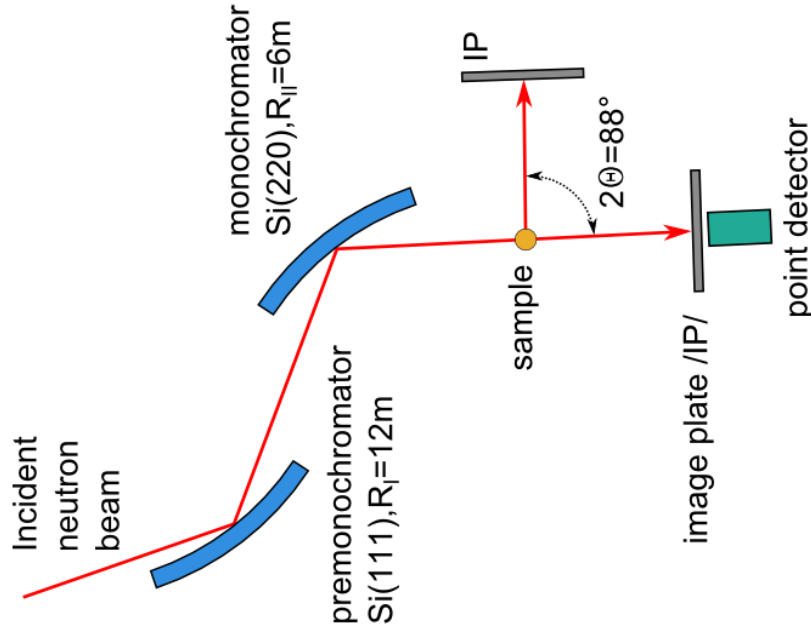
W. Woo, V. Em, G.B. An, P. Mikula and B.S. Seong, *Neutron diffraction residual stress measurements in a thick weld by using the wavelength with lower total cross-section*, Materials Science and Engineering A **528** (2011) 4120-4124.

V. Em, W. Woo, B.S. Seong, P. Mikula, J. Joo, M.H. Kang, K.H. Lee, *Residual stress determination in thick welded steel plates*, In Proc. of the ECNS 2011 Conf. 18-23, July, Journal of Physics: Conference Series, accepted.

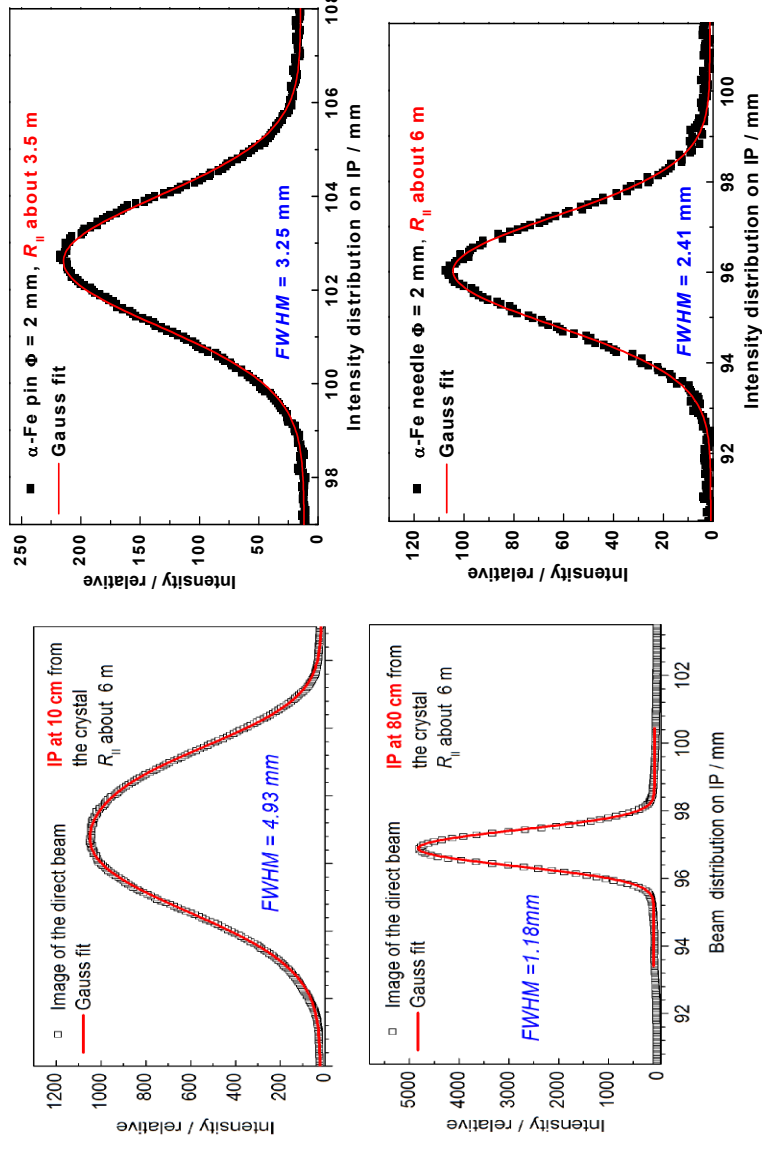


Two-dimensional mapping of the longitudinal residual stress (σ_x) in the 50 mm thick weld plate.

Unconventional neutron diffractometer

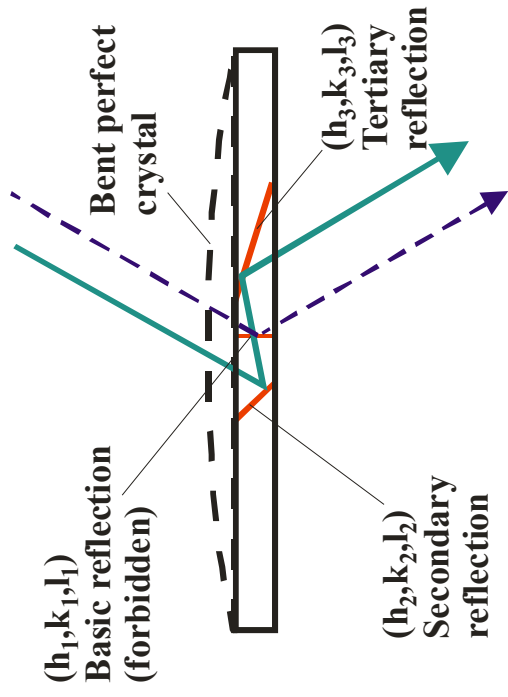


Schematic layout of the diffractometer permitting experiments in two or three axis mode.

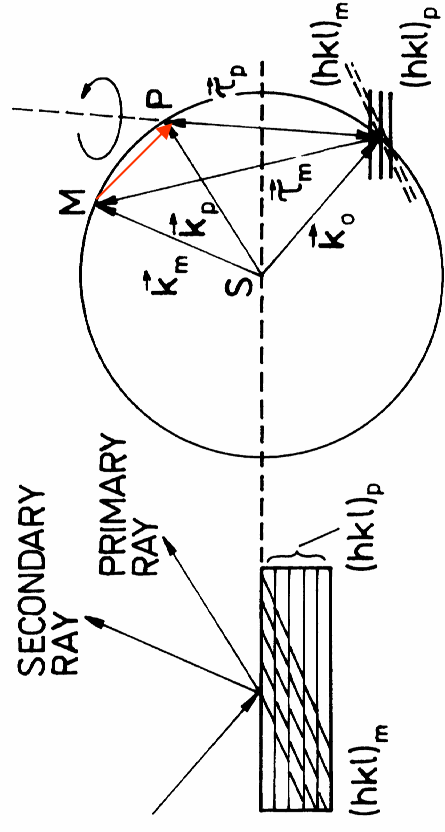


Profiles of the beam as taken by IP at 10 cm and 80 cm distance from the second crystal for $R_{II}=6\text{m}$ provide an evidence of a strong real space focusing.

Diffraction profiles of the beam as taken by IP from the α -Fe(211) polycrystalline sample situated at 50 cm from the Si(220) crystal and with IP at 45 cm from the sample for two different curvatures.



Schematic diagram of a simple double reflection process accompanying allowed or forbidden primary reflection.



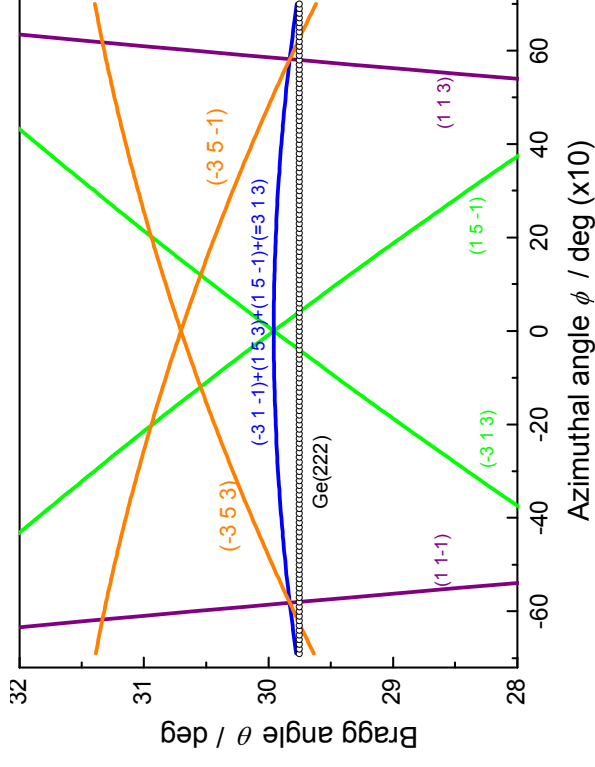
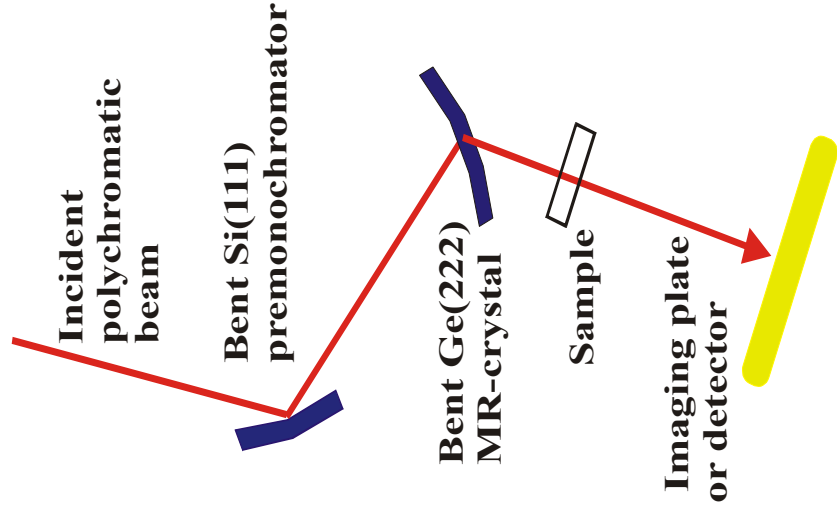
Momentum space representation of a MR-process

Relation for scattering vectors $\tau_p = \tau_m + \tau_m'$

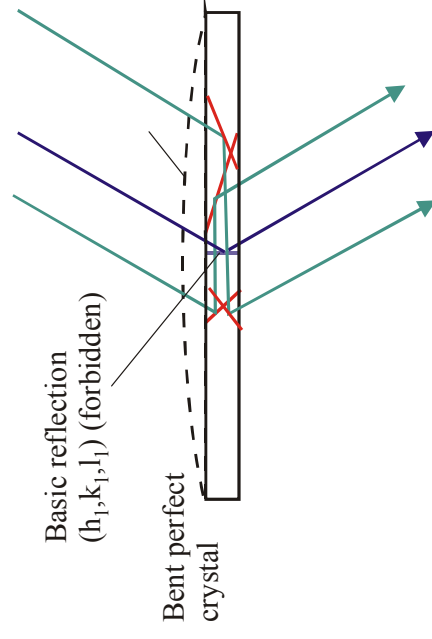
In the search of strong multiple Bragg reflection effects two methods are usually used:

- The method of azimuthal rotation of the crystal lattice around the scattering vector of the primary reflection for a fixed wave-length.
- The method of $\theta-2\theta_p$ scan in the white beam for a fixed azimuthal angle.

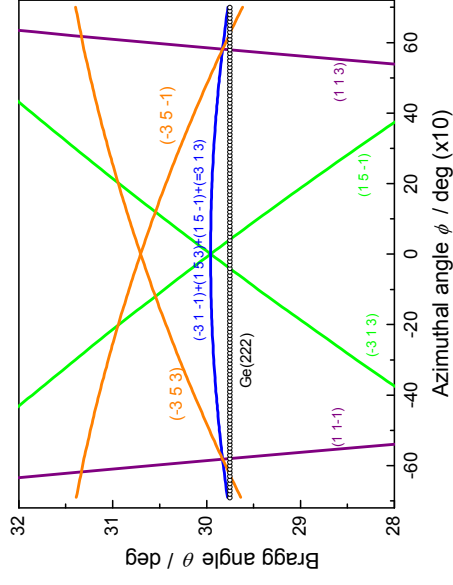
Neutron optics diffractometer in NPI Řež



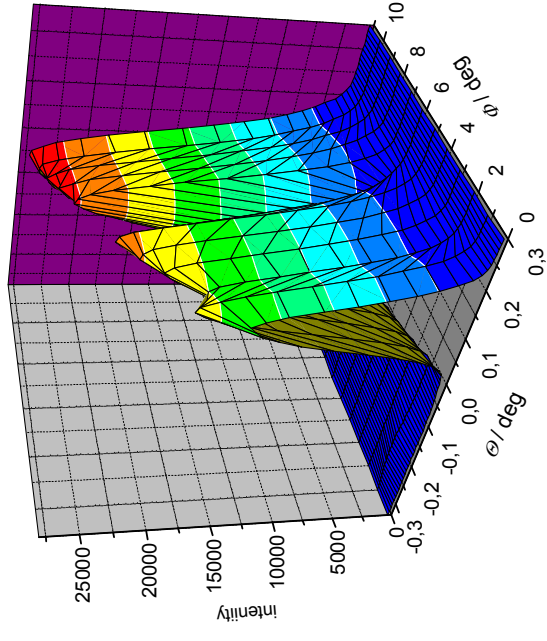
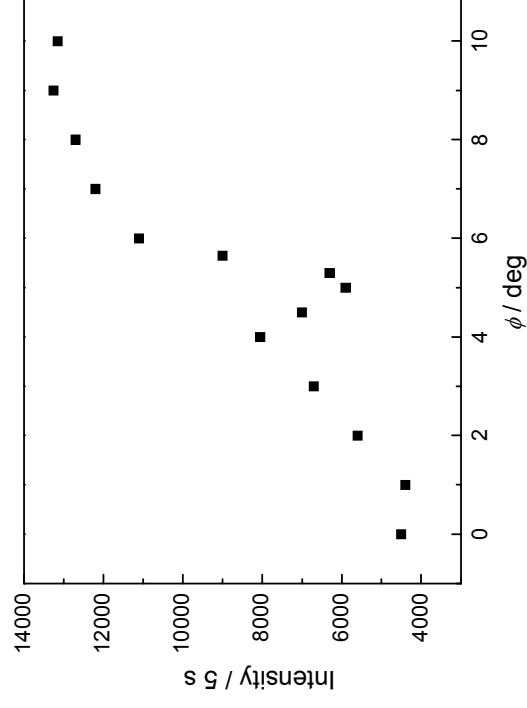
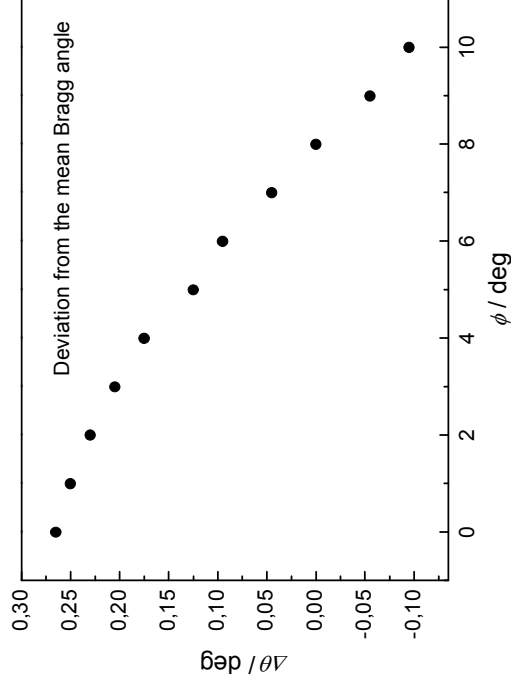
Part of the azimuth-Bragg angle relationship for 222 primary reflection of the diamond structure at the vicinity of the Bragg angle of 30°. Indexes are related only to secondary reflections.



Performance for searching MBR effect by the method of azimuthal rotation around the scattering vector of primary reflection and the three axis monochromator for an employment of MBR monochromator for diffraction experiment.



Experimental results of MR effects

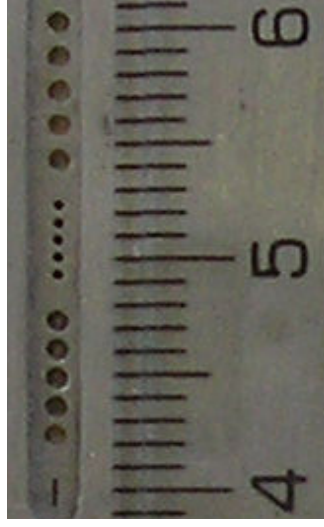


The 3-d intensity distribution constructed from the individual rocking curves for different azimuthal angles ϕ - (a), the peak intensities related to the rocking curves - (b) and the deviation of the rocking curve maxima from the mean Bragg angle 29.75° - (c).

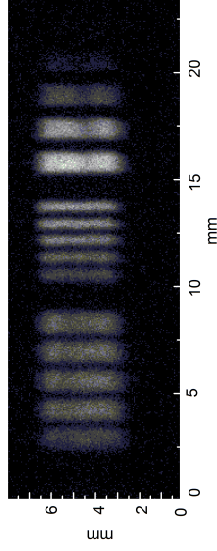
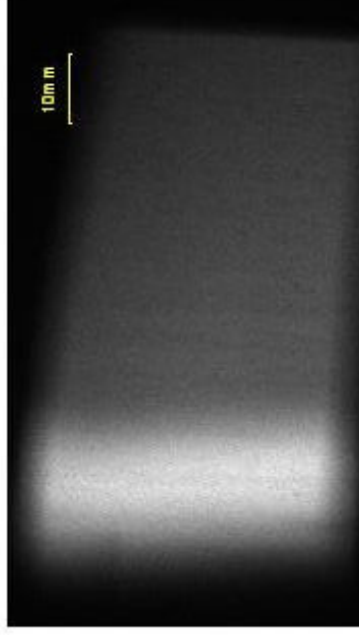
P. Mikula, M. Vrána, J. Šaroun, V. Em, B.S. Seong, *Investigation of multiple Bragg reflections at a constant neutron wavelength and their possible separation*, In Proc. of the ECNS 2011 conf. 18-23, July, Journal of Physics: Conference Series. Accepted.

P. Mikula, M. Vrána, J. Šaroun, V. Davydov, V. Em, B.S. Seong, *Experimental studies of dispersive double-reflections excited in cylindrically bent perfect-crystal slabs at a constant neutron wavelength*, J. Appl. Cryst., Accepted.

Experimental images



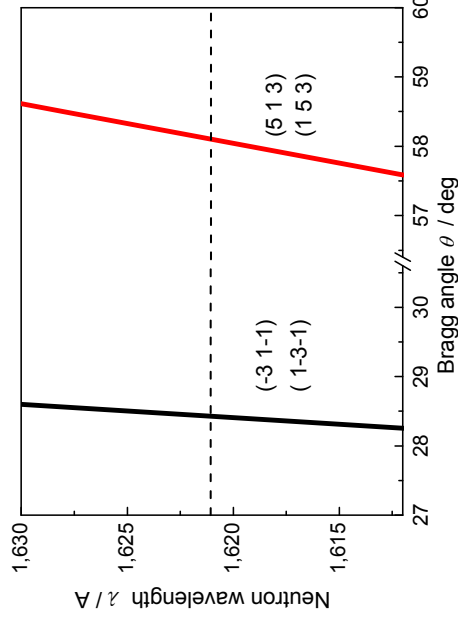
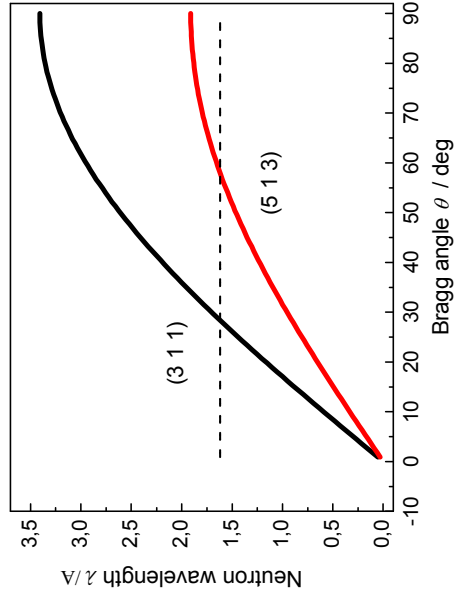
Width of IB
IB= 3 cm



Width of IB
IB= 6 mm

Photo of the holes of different diameters and their image taken by IP at 70 cm from the bent Ge crystal.

Image of the monochromatic beam obtained on the basis of the MR process.



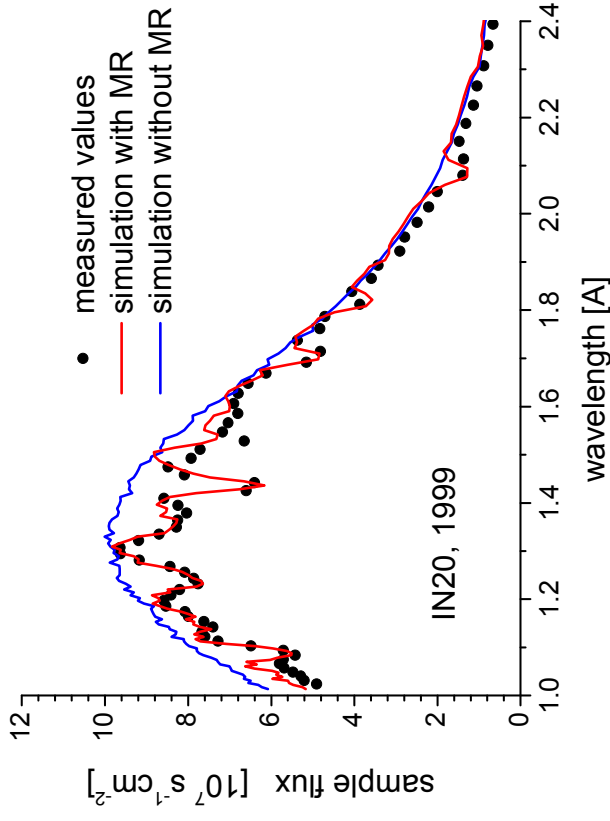
Bragg law for 311 and 513 reflections and enlarged part related to the MR process.

Monte Carlo simulation of parasitic and multiple Bragg reflections in elastically bent perfect crystals

Jan Šaroun, Jiří Kulda, Pavol Mikula, Miroslav Vrána

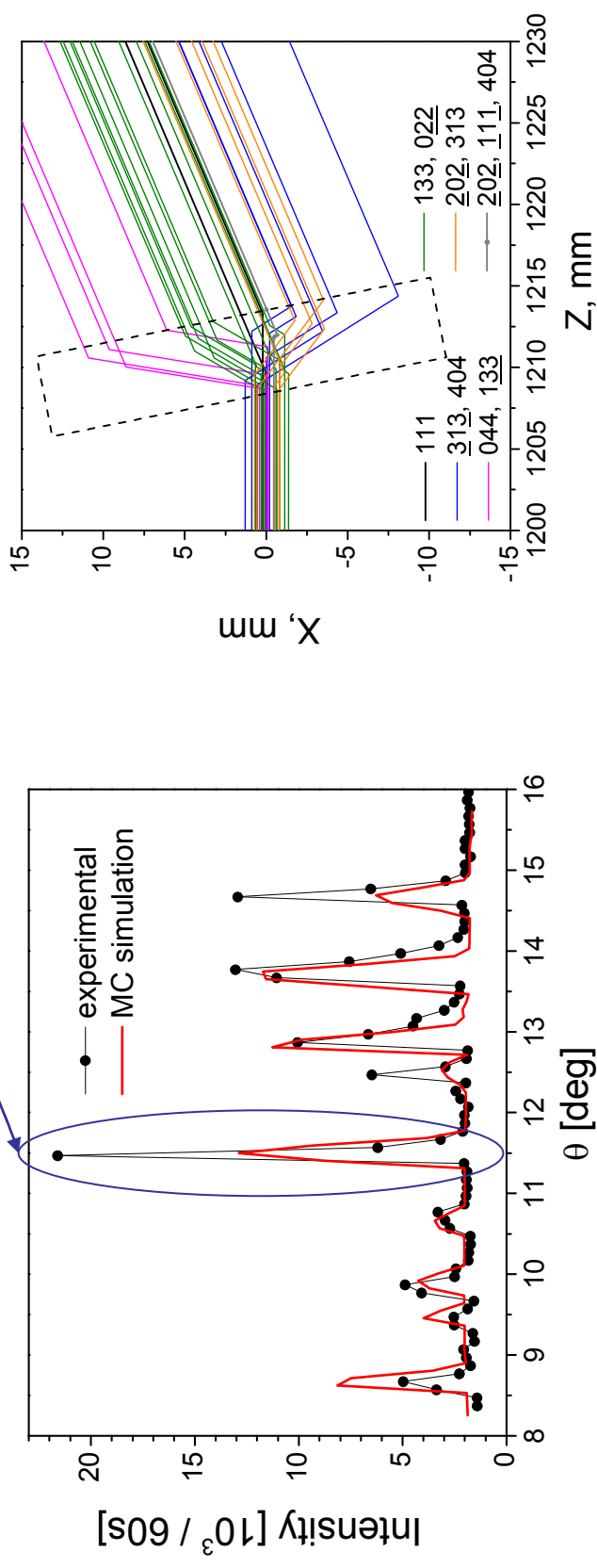
Lecture on NOP 2010 (Alpe d'Huez, March 17-19, 2010) *Nucl. Instr. and Meth. A* (2010), **634** (2011) S50-S54 (doi:10.1016/j.nima.2010.06.219)

- Single crystals of Si are used e.g. as neutron monochromators or transport medium at some types of multichannel focusing guide tubes (solid-state benders)
- **Multiple reflections** can appear in a **parasitic** way when decrease reflectivity of monochromators or transmission ability of neutron guides
- **New model** permits to predict **quantitatively** with a good precision **intensity of these effects** and thus better to optimize newly designed neutron optics elements of neutron diffractometers and spectrometers.



Comparison of the neutron flux spectrum distribution measured at the place of the sample position of the three axis spectrometer IN20 (ILL Grenoble, 1999) with the data obtained by a new model of MC simulations when including or not multiple reflections.

In the case of bent perfect crystals, *Umweganregung (MR effect)* may result in a considerable **strengthening of weak or forbidden reflections** and then permit possible applications in some diffraction experiments with high or ultrahigh resolution. MC simulation permits **quantitative calculations of intensities and spatial distributions of neutron trajectories** within the crystal.



One resulting reflection is composed of several double and triple reflections which are spatially separated (it is possible to see on the images of the reflected beam).